Title
STRAGGLING OF ENERGETIC HEAVY CHARGED PARTICLES IN THIN ABSORBERS

Author
Bichsel, Hans.

Publication Date
1969-09-01

Submitted to Physical Review

UCRL-19293
Preprint

STRAGGLING OF ENERGETIC HEAVY CHARGED PARTICLES IN THIN ABSORBERS

Hans Bichsel

September 1969

AEC Contract No. W-7405-eng-48

LAWRENCE RADIATION LABORATORY
UNIVERSITY of CALIFORNIA BERKELEY

STRAGGLING OF ENERGETIC HEAVY CHARGED PARTICLES IN THIN ABSORBERS*

Hans Bichsel

Lawrence Radiation Laboratory
University of California
Berkeley, California

September 1969

Abstract

The statistical fluctuations in the energy loss of heavy charged particles in thin absorbers due to collisions with atomic electrons are determined for collision cross sections obtained from the first Born approximation, using hydrogenic wavefunctions.

1. Introduction

This paper is a further extension of the derivation of straggling functions by Landau,[1] Vavilov,[2] Blunck and Leisegang,[3] and Shulek et al.[4] A better approximation to the true atomic collision cross sections is used at low energies, where the largest effects are expected.

The transport equation for the energy loss is

$$\frac{\partial f(x, \Delta)}{\partial x} = \int_0^{\infty} w(\epsilon) \times f(x, \Delta - \epsilon)\, d\epsilon - f(x, \Delta) \times \sigma_t , \qquad (1)$$

where $f(x, \Delta)$ is the probability density function of particles that have penetrated a thickness x of the absorber and have experienced an energy loss Δ, $w(\epsilon)\, d\epsilon$ is the differential collision cross section for single collisions, with an energy loss ϵ, and $\sigma_t = \int_0^{\infty} w(\epsilon)\, d\epsilon$ is the total collision cross section.

Equation (1) has recently been discussed by Tschalär[5] and Kellerer.[6] Collision cross sections are discussed in Section 2. It may be noted, though, that the true collision cross section $w(\epsilon)\, d\epsilon$ for single atoms is zero below an energy ϵ_{min} equal to the difference in energy between the lowest possible excited state and the ground state of the atoms, and also is zero for $\epsilon > \epsilon_{max} \approx 2mv^2$. Similarly, $f(x, \Delta - \epsilon)$ must be equal to zero for $\epsilon > \Delta$. The limits of integration introduced by Vavilov have to be understood from these conditions.

The solution of the transport equation using the Laplace transform[1,2] is

$$f(x, \Delta) = \frac{1}{2\pi i} \int_{c-i\infty}^{c+i\infty} \exp\left[p\Delta - x\int_0^\infty w(\epsilon)\,(1 - e^{-p\epsilon})\,d\epsilon\right] dp. \quad (2)$$

The derivation is discussed by Landau and Vavilov. Numerical methods are required for the evaluation of Eq. (2) for a general collision cross section. Vavilov[2] achieved an analytic form for the integral over ϵ, using $w(\epsilon) = k/\epsilon^2$, but performed a numerical integration for the integral over p. It should be noted that $c \to 0$ can be used in the limits. It is possible to express the solution for a general $w(\epsilon)$ in terms of a correction applied to the Vavilov solution. Therefore Vavilov's method is discussed in Section 3. Methods of performing the correction are discussed in Sections 4 and 5, and the modified straggling function is given in Section 6. Quantities calculated with $w(\epsilon) = k/\epsilon^2$ are denoted with primes, e.g., $f'(x, \Delta)$, I'_2.

2. The Atomic Collision Cross Sections

The practical results for straggling calculations so far have been obtained with the use of the classical electron cross section,[1, 2] modified by estimates[3, 4] of the influence of the "resonance effects" on the second moment M_2. The collision cross section $d\sigma'$ describing the collision of a heavy charged particle of charge ze, kinetic energy T, and velocity $v = \beta c$ with a free electron of mass m and charge -e is given by

$$d\sigma' = w(\epsilon)\,d\epsilon = k_1\epsilon^{-2}d\epsilon \qquad \text{for } \epsilon_e < \epsilon < \epsilon_m \quad (3)$$

$$d\sigma' = 0 \qquad \text{for all other } \epsilon,$$

where $k_1 = 2\pi z^2 e^4/mv^2$. Since we are concerned with low energies, a sufficient approximation for ϵ_m is given by $\epsilon_m = 2\,mv^2$. For the further applications in Eq. (13), the moments M'_n of $w(\epsilon) = k_1/\epsilon^2$ for $n > 1$ will be required. They are calculated for an absorber containing N atoms per cm^3 of atomic number Z,

$$M'_n = k\int_0^{\epsilon_m} \epsilon^{-2}\epsilon^m\, d\epsilon = k\,\epsilon_m^{n-1}/(n-1), \qquad (4)$$

where $k = k_1 NZ$, and $\epsilon_\ell = 0$, as assumed in the previous papers.

It is the intent of this paper to investigate the modifications necessary in the Vavilov theory caused by the use of more realistic collision cross sections. As a first, improved approximation, the values calculated with the first Born approximation,[7,8] using hydrogenic wave functions,[9,10] are used. Using Walske's notation,

$$d\sigma = k\, J\,(\eta, W)\, dW, \qquad (5)$$

where $W = \epsilon/(Z\text{-}d)^2 R_y$ is the energy ϵ lost by the particle expressed in suitable units, $\eta = mv^2/[\,2(Z\text{-}d)^2 R_y]$ is the energy of an electron having the same velocity as the incident particle; $R_y = 13.6$ eV is the Rydberg constant; d is a shielding factor for the nuclear charge of the absorber, depending on the electron shell; k is proportional to the number of electrons under consideration.

The excitation function J is defined by

$$J(\eta, W) = \int |\,F\,(\eta, \vec{q})\,|^2\, Q^{-2}\, dQ, \qquad (6)$$

where $\vec{q}$ is the change in momentum of the incident particle, $Q = q^2/2m$; $|\,F(\eta, \vec{q})\,|^2$ is the matrix element for the transition from the ground state to the excited state of energy W of the atom. Notice that the energy E of the secondary electron ("δ ray") is $E = \epsilon - I$, where I is the ionization energy of the atomic shell. The excitation functions have been recalculated for the K and L shells.[11] The difference between $w(\epsilon)$ and J can be appreciated from a plot of $d\sigma/d\sigma' = JW^2$ as a function of W. This is given in Figs. 1 and 2. The increase for small W corresponds to the resonance effects discussed by Bohr.[12] No simple analytic expression can be given for J or for its moments M_n:

$$M_n = k \int_{W_\ell}^{\infty} J(\eta, W)\, W^n\, dW. \tag{7}$$

The lower limit is now exactly the lowest possible excitation energy W_ℓ of the atomic shell, the upper limit can be set at ∞, because J drops off rapidly near $W_m = 4\,\eta = 2\,mv^2/(Z-d)^2 R_y$. It is to be expected, though, that, for large η, the tail beyond $4\,\eta$ (see Figs. 1 and 2) will contribute increasingly to the higher moments.

The total collision cross section σ_t, equal to the moment M_0, has been discussed, e.g., by Merzbacher and Lewis[13] and by Brandt and Laubert.[14] The stopping power S, equal to the first moment M_1, is discussed in many papers.[9, 15] The stopping number $B = M_1/k$ is compared with the expression $\ell n\ 2\,mv^2/I$, used frequently in simplified stopping power theory, in Fig. 3.

An approximation for the second moment has been given in Livingston and Bethe;[16] for the higher moments, $M_n = M'_n$ is usually chosen. This is not a good assumption, as mentioned above. The second and third moments for the L shell are given in Figs. 4 and 5; some higher moments are listed in Table I.

For solids, the excitation function for valence electrons will be modified for energy losses below 50 or 100 eV by a resonance-type cross-section curve,[17, 18] with a finite slope toward low energies. For single atoms, extremely steep slopes are expected in the cross section at energy losses equal to the excitation energies.[19] Although these effects are quite important for σ_T and S, they produce relatively small changes in the higher moments M_2, M_3, $\cdots$.

3. The Vavilov Solution

In order to solve Eq. (2) it will be useful to consider separately the integral over ϵ:

$$I_1 \equiv \int_0^\infty w(\epsilon)\,(1 - e^{-p\epsilon})\,d\epsilon \,. \tag{8}$$

Since p is imaginary, I_1 is complex. In general, the uncertainty in the knowledge of $w(\epsilon)$ is greater at small values of ϵ. Landau and Vavilov therefore extract the first moment M_1 of $w(\epsilon)$ from I_1,

$$M_1 \equiv \int w(\epsilon)\,\epsilon\,d\epsilon, \tag{9}$$

by adding and subtracting $p\epsilon$ in the parenthesis:

$$I_1 = p\int w(\epsilon)\,\epsilon\,d\epsilon + \int w(\epsilon)\,(1 - e^{-p\epsilon} - p\epsilon)\,d\epsilon, \tag{10}$$

with

$$I_2 \equiv \int w(\epsilon)\,(1 - e^{-p\epsilon} - p\epsilon)\,d\epsilon, \tag{11}$$

and, since M_1 is the stopping power S of the material, we obtain

$$I_1 = pS + I_2. \tag{12}$$

The behavior of $w(\epsilon)$ at small values of ϵ is less important in I_2, and for S, an experimental value can be chosen, thus eliminating uncertainties in $w(\epsilon)$ for the first moment. For the method described in Section 5, the power-series expansion of I_2 will be needed:

$$I_2 = - \sum_{n=2}^{\infty} (-1)^n \frac{p^n}{n!} \int w(\epsilon)\, \epsilon^n\, d\epsilon = - \sum_{n=2}^{\infty} (-1)^n \frac{p^n M_n}{n!}, \qquad (13)$$

where the $M_n = \int w(\epsilon)\, \epsilon^n\, d\epsilon$ (see also Eqs. 4 and 7) are the moments[3, 6] of the collision cross section spectrum $w(\epsilon)$.

The evaluation of Eq. (11) using the free-electron collision spectrum has been given by Vavilov and is repeated here. The real and imaginary parts, $\Re(I'_2)$ and $\Im(I'_2)$, are written separately, with $p = i\,y$, $t = y\,\epsilon_m$:

$$\Re(I'_2) = k \int_0^{\epsilon_m} \frac{1-\cos y\epsilon}{\epsilon^2}\, d\epsilon = k\,y \left[\frac{\cos t - 1}{t} + \mathrm{Si}(t)\right] \qquad (14)$$

$$= \frac{k}{\epsilon_m} \left[\cos t - 1 + t\,\mathrm{Si}(t)\right],$$

where $\mathrm{Si}(t) \equiv \int_0^t \frac{\sin t'}{t'}\, dt'$; $\mathrm{Si}(0) = 0$,

$$\Im(I'_2) = k \int_0^{\epsilon_m} \frac{\sin y\epsilon - y\epsilon}{\epsilon^2}\, d\epsilon = \frac{k}{\epsilon_m} \left\{ t - \sin t + t[\mathrm{Ci}(t) - \ln t - \gamma] \right\}, \qquad (15)$$

where $\mathrm{Ci}(t) \equiv \int_0^t \frac{\cos t' - 1}{t'}\, dt' + \ln t + \gamma$, for $\gamma = 0.577216$. (16)

The functions $\Re$ and $\Im$ are plotted in Figs. 6 and 7 for several values of ϵ_m.

For an arbitrary collision spectrum $w(\epsilon)$, two procedures can be used to determine I_2:

(a) direct numerical evaluation of Eq. (11), discussed in Section 4,

(b) calculations based on the use of Eq. (13), similar to the methods used in Refs. 3 and 4; discussed in Section 5.

4. The Transform of the Quantum-Mechanical Collision Cross Sections

The integral I_2 defined in Eq. (11) has been calculated numerically for the collision cross section J(W) defined in Section 2 for a number of purely imaginary values of p, $0 < |p| < 1000$. Since only a limited number of values of J(W) are available at $W = W_n$, $n = 1, 2, 3 \cdots$, and since $(1-e^{-p\epsilon} - p\epsilon)$ oscillates rather strongly, the mean value theorem has to be used for the integral:

$$I_2(p, \eta) \approx k \sum_n J(W_n, \eta) \int_{a_n}^{b_n} (1 - e^{-pW} - pW)\, dW =$$

$$k \sum_n J(W_n, \eta) \left[b_n - a_n + p^{-1}(e^{-pa_n} - e^{-pb_n}) - \frac{p}{2}(a_n^2 - b_n^2) \right] , \qquad (17)$$

where $a_n = (W_n W_{n-1})^{1/2}$, $\qquad b_n = (W_n W_{n+1})^{1/2}$,

since the W_n follow a geometrical progression. The ratios $r = \mathcal{R}(I_2)/\mathcal{R}(I'_2)$ and $r_i = \mathcal{J}(I_2)/\mathcal{J}(I'_2)$ are given in Figs. 8 and 9 for L-shell electrons. The numerical accuracy of the results can be estimated from a comparison of the evaluation of Eq. (17), using $J' = 1/W^2$, with results calculated with Eqs. (14) and (15). The agreement is within 0.1%; a slightly larger error for I_2 is expected because of the faster change of J(W) at small W.

For very small values of p, I_2 can be written as

$$\mathcal{R}(I_2) \approx -p^2 M_2/2, \tag{18}$$

$$\mathcal{J}(I_2) \approx p^3 M_3/6i, \tag{19}$$

derived from Eq. (13), and therefore $\mathcal{R}(I_2)/\mathcal{R}(I'_2) \approx M_2/M'_2$ and $\mathcal{J}(I_2)/\mathcal{J}(I'_2) \approx M_3/M'_3$.

5. The Method of Moments

The direct evaluation of Eq. (13) is not practical, because quite a large number of terms would have to be calculated. Blunck and Leisegang[3] and Shulek et al.[4] suggested the comparison of M_2 with the moment M'_2 of the free-electron cross section. This method can readily be extended to all moments. Using $\delta_n \equiv M_n - M'_n$, with M_n from Eq. (7) and M'_n from Eq. (4), we obtain

$$I_2 = -\sum_{n=2}^{\infty} (-1)^n M'_n\, p^n/n! - \sum_{n=2}^{\infty} (-1)^n p^n \delta_n/n! \tag{20}$$

The first sum is exactly I'_2, and the last sum therefore is the contribution due to the difference in the higher moments of the true collision cross section from the free-electron value $1/\epsilon^2$. It is convenient to introduce

$D_n = \delta_n/M'_n = (M_n/M'_n) - 1$ to modify the second sum:

$$-S_2 \equiv \sum (-1)^n p^n \delta_n/n! = k\sum (-1)^n p^n \epsilon_m^n D_n/[n!(n-1)\epsilon_m] . \quad (21)$$

D_n can be obtained from Figs. 4 and 5 and Table I.

Using the substitution $p = it/\epsilon_m$, we obtain

$$-S_2 = \epsilon_m^{-1} k \sum_{n=2}^{\infty} (-1)^n (it)^n D_n/[n!(n-1)] . \quad (22)$$

Shulek et al.[4] have used this approach, introducing only a second moment $M_2 = k[\epsilon_m' Z_{eff}/Z + \sum_i 2.667 I_i f_i \ln(\epsilon_m/I_i)]$, first discussed in Ref. 16, to get a second approximation to I_2. Corresponding curves, using the more appropriate second moments from Fig. 4, are shown in Fig. 8, for $\eta_L = 1.5$ and 10. Since the region $1 < p < 10$ is still quite important for the convergence of Eq. (2) (see Fig. 14), this procedure is usually not satisfactory. The imaginary part is unchanged, since it does not contain M_2. The use of higher moments in Eq. (20) leads to problems; D_4 is quite small (Table I), whereas the higher moments give larger contributions and lead to wild fluctuations of S_2 for p above 0.5 or 1.0. As elegant as the method may appear, it is not practical.

6. Modifications of the Vavilov Function

With the function I_2 defined in Eq. (11), it is now possible to write Eq. (2) in the form

$$f(x, \Delta) = \frac{1}{2\pi i} \int_{-i\infty}^{i\infty} e^{p[\Delta - \bar{\Delta}] - xI_2} \, dp, \quad (23)$$

where $\bar{\Delta} = xS$ is the mean energy loss of a beam of particles. Further, using $\kappa = xk/\epsilon_m$ and $p = it/\epsilon_m$, we have

$$f(x, \Delta) = \frac{1}{2\pi\ \epsilon_m} \int_{-\infty}^{\infty} \exp\left\{ it \frac{(\Delta-\bar{\Delta})}{\epsilon_m} - \kappa r[\cos t - 1 + t\,\mathrm{Si}(t)]\right.$$

$$\left. - i\kappa\ r_i[t - \sin t + t\,(\mathrm{Ci}(t) - \ell n\, t - \gamma)]\right\} dt \qquad (24)$$

$$= \frac{\kappa}{\pi\xi} \int_0^{\infty} \exp\left\{-\kappa\, r\,[\cos t - 1 + t\,\mathrm{Si}(t)]\right\}$$

$$\times \cos\left\{t\left[\frac{\Delta-\bar{\Delta}}{\epsilon_m}\right] + \kappa\ r_i\ [t\gamma - t + \sin t + t\ \ell n\, t - t\,\mathrm{Ci}(t)]\right\} dt.$$

Note that the imaginary part of the integral is antisymmetric in t and therefore does not contribute to the integral. For $r = r_i = 1$, Eq. (24) is exactly Vavilov's expression [Eq. (V-16)] for $\beta^2 = 0$. The terms containing β^2 in Eq. (V-16) appear because of the choice of $w(\epsilon) = k\,\epsilon^{-2}(1-\beta^2\epsilon/\epsilon_m)$ by Vavilov. This relativistic correction factor has been neglected here because the excitation function J(W) is nonrelativistic. Notice that the factor e^{κ} outside of the integral in Eq. (V-16) is not constant in Eq. (24).

The function $f(x, \Delta)$ has been calculated for several values of κ for the values of η_L given in Fig. 8. The results are given in Figs. 10-13. For comparison, the Vavilov curves and curves including the correction for the second moment (Shulek et al.) are also given.

An impression of the problems encountered in the numerical integration of Eq. (24) can be obtained from a plot of the integral as a function of the upper limit. An example is shown in Fig. 14.

7. Comments and Conclusions

Straggling functions derived from the transport equation with the use of collision cross sections calculated in the first Born approximation, with hydrogenic wavefunctions, are discussed. Substantial deviations from the Vavilov functions and the functions modified by Shulek et al. are found, especially for low energy particles in thin absorbers. Further improvements in the theoretical treatment require better collision cross sections. For the general use of the procedure suggested here, it is necessary to calculate the contributions for all the shells of a given absorber. No reliable collision cross sections for the higher shells are presently available. A scaling procedure with adjustable parameters similar to the method used for the "shell corrections" in stopping power[15] or, alternatively, collision cross sections calculated from a statistical model of the atom,[20] might be used.

Existing experimental data[21-25] are not at suitable energies, or, in general, accurate enough to confirm the trends discussed here.

For future straggling measurements, it will probably be necessary to determine the first moment (the stopping power) and the second moment (the standard deviation) from the experiment. The third and fourth moments deviate only little from the free-electron moments and probably cannot be determined experimentally with sufficient accuracy to distinguish between the two theories. For the higher moments, even very small amounts of slit edge scattering, nuclear reactions, etc., contribute heavily to the experimental probability densities. The derivation of further details of the collision cross sections from straggling measurements thus does not appear promising, except maybe in extremely thin absorbers,[18] with only a few collisions per particle. For this type of experiment, Kellerer's convolution method would be more suitable[6] for the analysis.

Table I. Higher moments M_n of the quantum mechanical collision cross section. M_n depend very little on W_m.

	n						
η_L	4	5	6	7	8	9	10
0.1	1.08	1.97	4.57				
0.2	1.04	1.51	2.65				
0.25	1.026	1.42	2.30	4.62	26.2	1926	—
0.4	1.012	1.27	1.80				
0.9	1.003	1.12	1.35				
1.5	1.001	1.074	1.210	1.434	1.821	2.85	25.5
4	1.0005	1.03	1.08				
10	1.0005	1.01	1.032	1.061	1.102	1.16	1.24
20	1.0005	1.01	1.016				
40	1.0005	1.003	1.008				
100	1.000	1.000	1.002	1.004	1.008	1.0115	1.016

*Work supported in part by the U. S. Atomic Energy Commission and Public Health Service Research Grant No. CA-08150 from the National Cancer Institute.

1. L. Landau, USSR J. Phys. 8, 201 (1944).
2. P. V. Vavilov, Sov. Phys.--JETP 5, 749 (1957).
3. O. Blunck and S. Leisegang, Z. Phys. 128, 500 (1950).
4. P. Shulek, B. M. Golovin, L. A. Kulyukina, S. V. Medved, and P. Pavlovich, Sov. J. Nucl. Phys. 4, 400 (1967).
5. C. Tschalär, Nucl. Instr. Methods 61, 141 (1968).
6. A. Kellerer, G. S. F. Bericht B-1 (November 1968) Strahlenbiologisches Institut der Universität München.
7. U. Fano, Penetration of Protons, Alpha Particles, and Mesons, Ann. Rev. Nucl. Sci. 13, 1 (1963).
8. H. Bethe, Ann. Physik 5, 325 (1930).
9. M. C. Walske, Phys. Rev. 88, 1283 (1952); Phys. Rev. 101, 940 (1956).
10. G. S. Khandelwal and E. Merzbacher, Phys. Rev. 144, 349 (1966); Phys. Rev. 151, 12 (1966).
11. Unpublished calculations by the author, available on computer tape. Approximate values can be obtained from Figs. 1 and 2.
12. N. Bohr, Kgl. Danske Videnskab. Selskab. Mat.-Fys. Medd. 18, [8] (2nd ed,) (1953).
13. E. Merzbacher and H. W. Lewis, In Encyclopedia of Physics, S. Flügge, ed., Vol. 34, (Springer-Verlag, Berlin, 1958).
14. W. Brandt and R. Laubert, Phys. Rev. 178, 225 (1969).

15. H. Bichsel, Passage of Charged Particles Through Matter, American Institute of Physics Handbook, 3d ed. (to be published).

16. M. S. Livingston and H. Bethe, Rev. Mod. Phys. 9, 263 (1957).

17. P. Nozières and D. Pines, Phys. Rev. 113, 1254 (1959).

18. R. E. Burge and D. L. Misell, Phil. Mag. 18, 251 (1968).

19. J. T. Park and F. D. Schowengerdt, Rev. Sci. Instr. 40, 753 (1969).

20. E. Bonderup, Kgl. Danske Videnskab. Seskab Mat.-Fys. Medd. 35, [17] (1967).

21. T. J. Gooding and R. M. Eisberg, Phys. Rev. 105, 357 (1957).

22. L. P. Nielsen, Kgl. Danske Videnskab. Selskab Mat.-Fys. Medd. 33 [6] (1961).

23. H. D. Maccabee, M. R. Raju, and C. A. Tobias, Phys. Rev. 165, 469 (1968).

24. J. J. Kolata, T. M. Amos, and Hans Bichsel, Phys. Rev. 176, 484-489 (1968).

25. D. W. Aitken, W. L. Lakin, and H. R. Zulliger, Phys. Rev. 179, 393 (1969).

Figure Captions

Fig. 1. The excitation function J_K for the K shell. Plotted is the product $J_K W^2$, where W is the electron energy in atomic units: $W = \epsilon(eV)/13.6\times(Z-0.3)^2$. The parameter $\eta_K = 18\,800\ \beta^2/(Z-0.3)^2$ is equal to the energy (in atomic units) of an electron of the same velocity $v = \beta c$ as the incident particle. The energy $\epsilon_{max} = 2\ mv^2$ for a free electron corresponds to $W_{max} = 4\eta_K$. The lower limit for the integrals is $W_{min} = I_K(eV)/13.6\times(Z-0.3)^2$, where I_K is the energy to lift a K-shell electron to the lowest unoccupied level of the atom with atomic number Z (a relativistic correction is neglected here). The asymptotic value is $JW^2 \rightarrow 1$.

Fig. 2. The product $J_L W^2$ for the L shell. The units are the same as defined for the K-shell, except that $(Z-0.3)^2$ is to be replaced by $(Z-4.15)^2$. Notice that J_L as well as J_K extends beyond $4\eta_L$: there is a small probability of collisions for energies $\epsilon > 2\ mv^2$. W_{min} depends on Z: for Al, $W_{min} \approx 0.0926$, for Pb, $W_{min} \approx 0.167$. The asymptotic value of $J_L W^2$ is 4.

Fig. 3. The stopping number B_L as a function of η_L for $Z \approx 50$, compared with $B_L' = 3.37\times \ln(2\ mv^2/I_L)$. The shell correction C_L is the difference between B_L and B_L': $C_L = B_L - B_L'$.

Fig. 4. The ratio $r_2 = M_2/M_2'$ of the quantum mechanical and the free electron cross sections for the L shell. The four curves are drawn for $W_\ell \equiv W_{min} = 0.093$ (silicon), 0.115 (copper), 0.135 (silver) and 0.167 (lead). For $\eta_L > 4$, the expression of Ref. 16 agrees approximately with the curves given here, but deviates strongly at smaller η_L.

Fig. 5. The ratio $r_3 = M_3/M_3'$ for the L shell. The same values for W_{min} are used as for Fig. 4.

Fig. 6. The real part $\Re(I_2')$ of the integral I_2' for three values of $W_m = 4\eta_L$, as a function of the Laplace transform parameter y. The electron energies corresponding to W_m are $\epsilon_m = W_m \times 13.6$ eV $(Z-4.15)^2$. The dotted line is $\Re(I_2)$, when the quantum-mechanical collision cross section is used, for $\eta_L = 10$. This function is the exponent in the integrand of Eq. (24).

Fig. 7. The imaginary part of the integral I_2' for three values of W_m. The dotted lines show the function for I_2. This function, added to $y(\Delta - \bar{\Delta})$, forms the argument of the cos in Eq. (24).

Fig. 8. The ratio r of the real part of I_2 and the real part of I_2'. The dotted lines indicate the correction by Shulek et al. (Ref. 4).

Fig. 9. The ratio $r_i = \Im(I_2)/\Im(I_2')$ of the imaginary part of I_2 and I_2'.

Fig. 10. Straggling function $f(x, \Delta)$ for low energy particles in a thin detector. The abscissa is $\lambda = (\Delta - \bar{\Delta})/xk + \langle\lambda\rangle$ where $\langle\lambda\rangle = 0.577216 - \beta^2 - 1 - \ell n\,\kappa$. The solid line represents results of my theory, the dotted line is the Vavilov curve for $\beta^2 = 0$. The difference for a slightly larger β^2 is very small. The full width at half maximum (fwhm) of f' is 11% larger than that of f. Example: protons in an argon-filled counter. With $\eta_L = mv^2/[2 R_y (Z-4.15)^2] \approx 40\ T(\text{MeV})/(Z-4.15)^2$, the energy of the proton is about 1.2 MeV. Since $\kappa = 1$, $x \approx 0.02$ mg/cm^2 or 1 cm at about 40 torr. The mean energy loss amounts to about 3 keV, and would be affected seriously by δ-ray escape. The narrowing of the straggling curve predicted here for the L shell would be

partially compensated by a widening contributed by the M-shell electrons.

Fig. 11. Straggling function $f(x, \Delta)$ for L-shell electrons at $\eta_L = 1.5$ (solid line). This is approximately the energy giving the maximum quantum mechanical effect (see Fig. 4). The fwhm of $f(x, \Delta)$ is about 34% wider than that of $f'(x, \Delta)$. Since the area under the curve [equal to the moment $M_0 = \int f(x, \Delta)\, d\Delta$] is not very sensitive to the contributions from the tails of the function, the peak height of the normalized function from an experiment gives important information. To find it, determine the number of particles occurring in the peak channel (the spectrum is assumed to be measured in a multichannel analyzer) as a fraction of the total number of particles in the spectrum, multiply it with xk/c, where c is the width of a channel in the same units as xk, and compare with the maximum value of $f(x, \Delta)$. The measurement of fwhm or the determination of the standard deviation is more sensitive, though.

Fig. 12. Medium-energy particles in a thin detector (e. g., ≈ 25-MeV protons in a silicon detector of thickness $x \approx 3.7\ \mathrm{mg/cm^2}$ with $\overline{\Delta} \approx 63$ keV). My theory: solid line; Vavilov theory for $\beta^2 = 0$: dotted line. The theory by Shulek et al. differs by only a few percent from the solid line. The ratio of the fwhm is 1.12.

Fig. 13. Similar to Fig. 11, for $\kappa = 1$. This would apply to 4-MeV protons in a silicon detector of $1\ \mathrm{mg/cm^2}$, $\overline{\Delta} \approx 70$ keV. The ratio of the fwhm is about 1.05, the ratio of the peaks is about the same.

Fig. 14. The integral of the inverse Laplace transform for the straggling function $f(x, \Delta)$, Eq. (24), as a function of the upper limit, for $\kappa = 0.1$, and $\lambda = 12.3$. The solid line is used for the function with the quantum-mechanical cross section, the dotted line for the free electron cross section. The large oscillation for $p < 1$ requires great care in the numerical integration to avoid errors in the relatively small value of the integral. For smaller values of λ, the oscillations are less important.

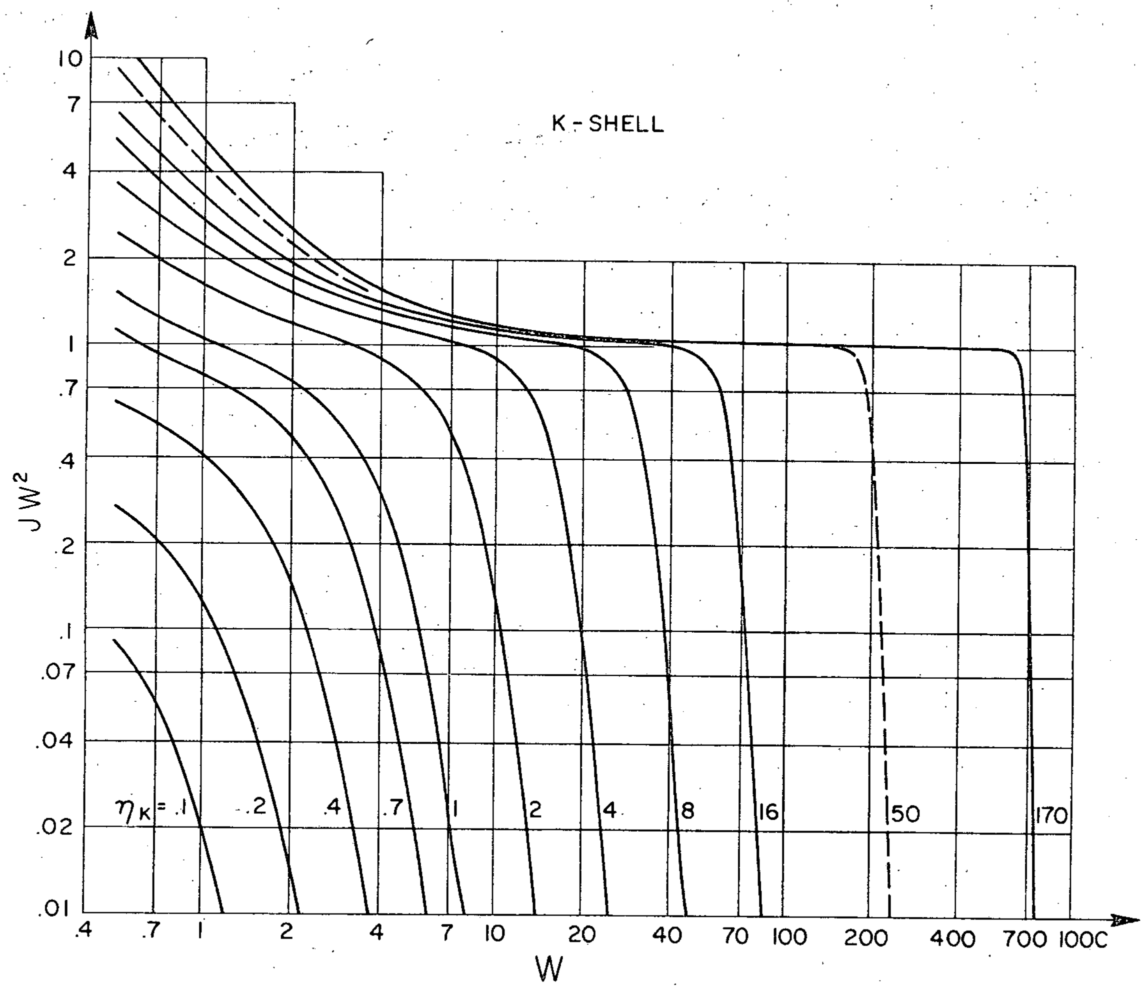

XBL 699-1465

Fig. 1

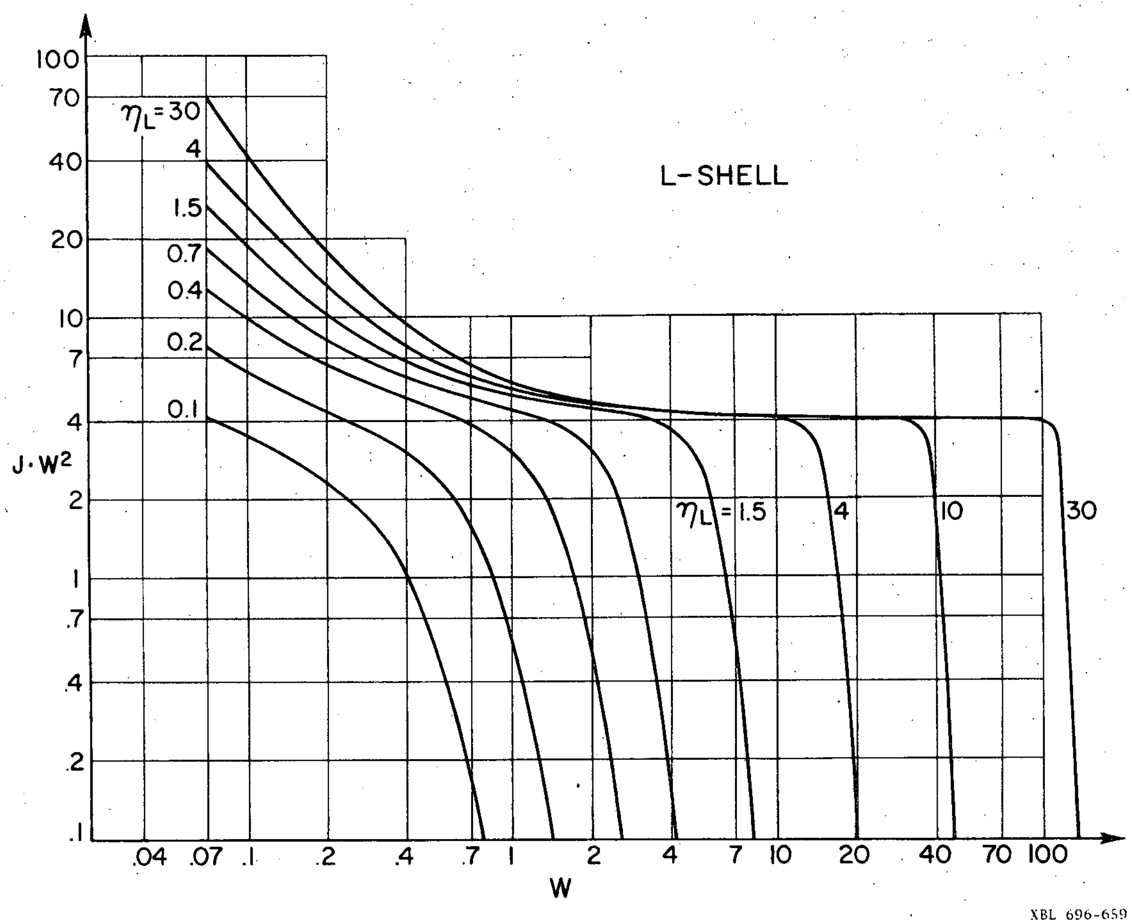
L-SHELL
η_L=30
4
1.5
0.7
0.4
0.2
0.1
η_L=1.5
4
10
30
J·W²
W
100
70
40
20
10
7
4
2
1
.7
.4
.2
.1
.04 .07 .1 .2 .4 .7 1 2 4 7 10 20 40 70 100
XBL 696-659

Fig. 2

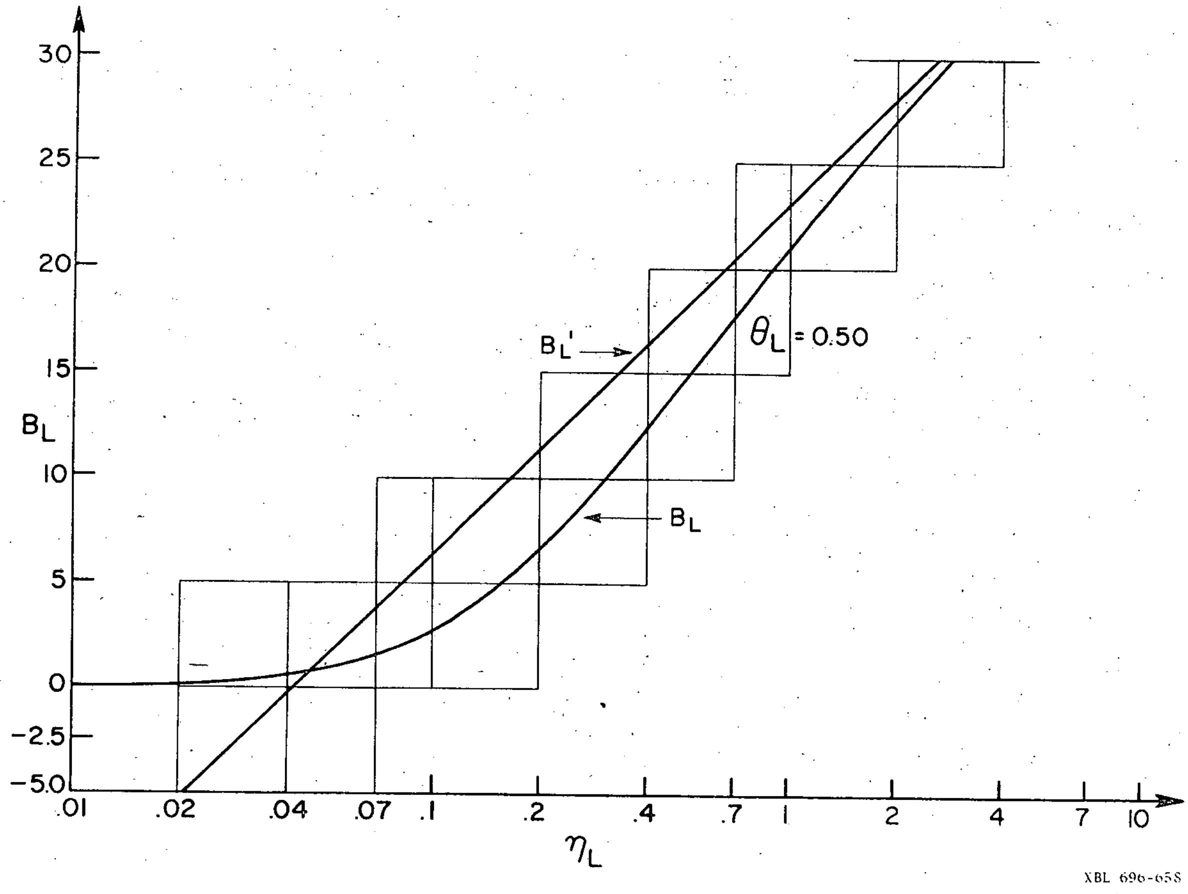
30
25
20
15
10
5
0
−2.5
−5.0
B_L
B_L'
B_L
$\theta_L = 0.50$
.01
.02
.04
.07
.1
.2
.4
.7
1
2
4
7
10
η_L
XBL 696-658

Fig. 3

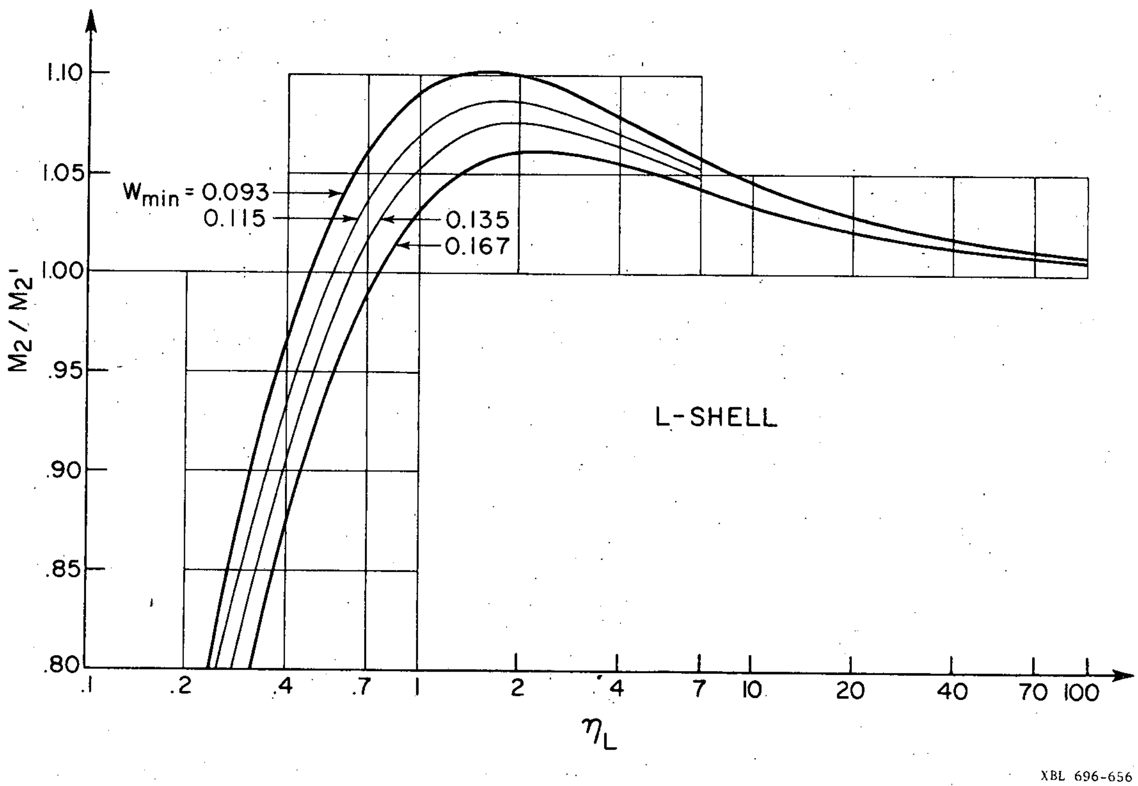
1.10
1.05
1.00
.95
.90
.85
.80
M2 / M2'
W$_{min}$ = 0.093
0.115
0.135
0.167
L-SHELL
.1
.2
.4
.7
1
2
4
7
10
20
40
70
100
η_L
XBL 696-656

Fig. 4

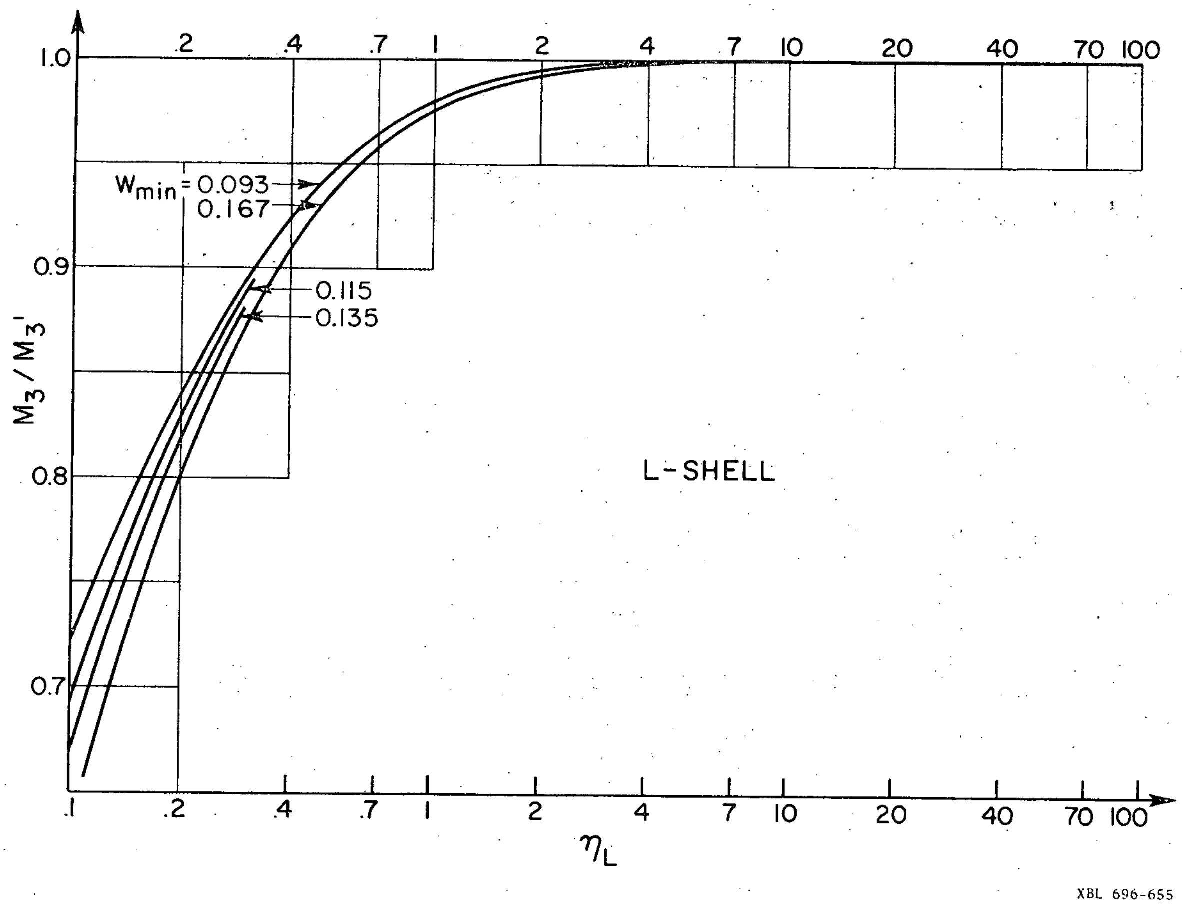
1.0
0.9
0.8
0.7
M_3 / M_3'
.1
.2
.4
.7
1
2
4
7
10
20
40
70
100
η_L
W_{min} = 0.093
0.167
0.115
0.135
L-SHELL
XBL 696-655

Fig. 5

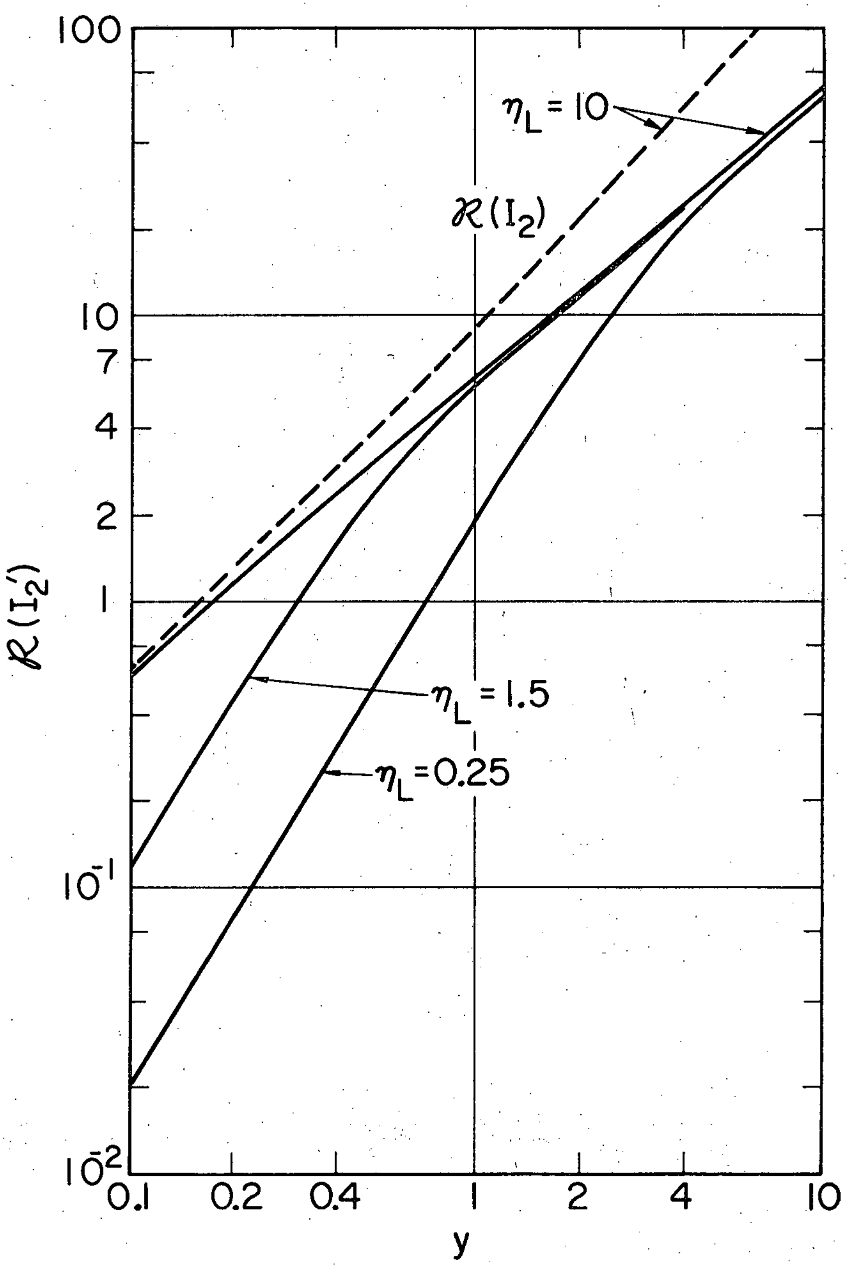

XBL698-3444

Fig. 6

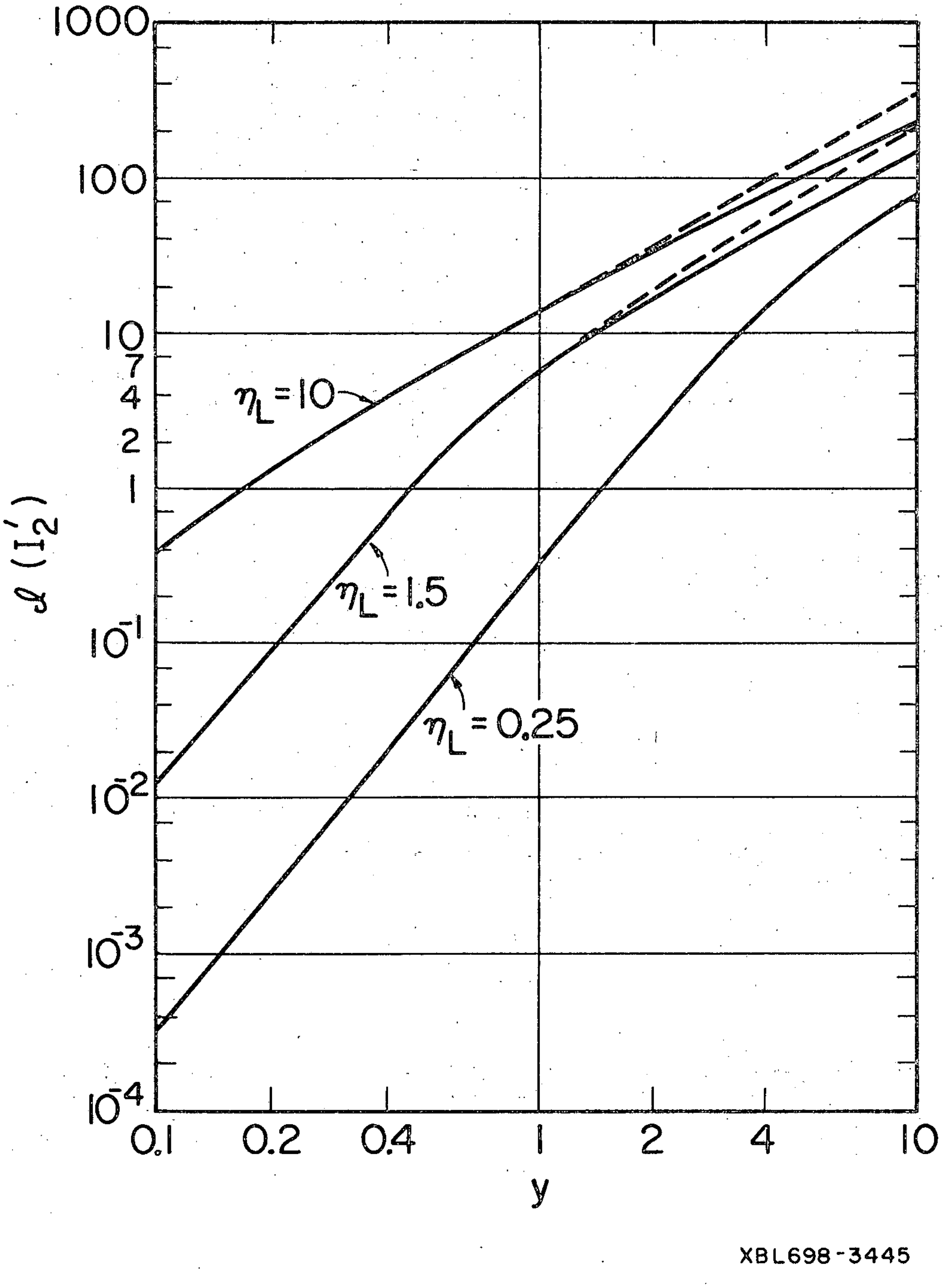
1000
100
10
7
4
2
1
10^{-1}
10^{-2}
10^{-3}
10^{-4}
$\ell(I_2')$
$\eta_L = 10$
$\eta_L = 1.5$
$\eta_L = 0.25$
0.1
0.2
0.4
1
2
4
10
y
XBL698-3445

Fig. 7

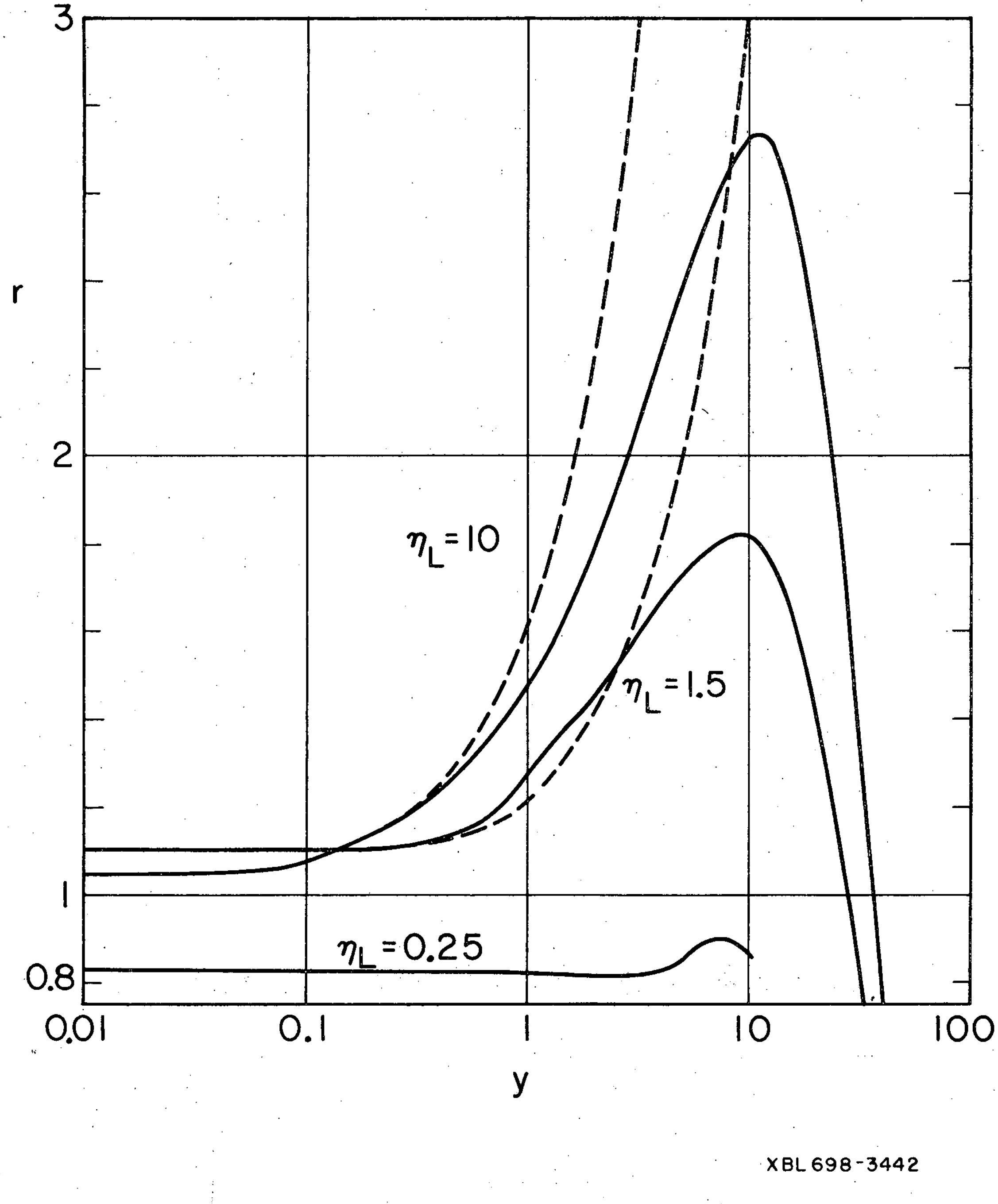

Fig. 8

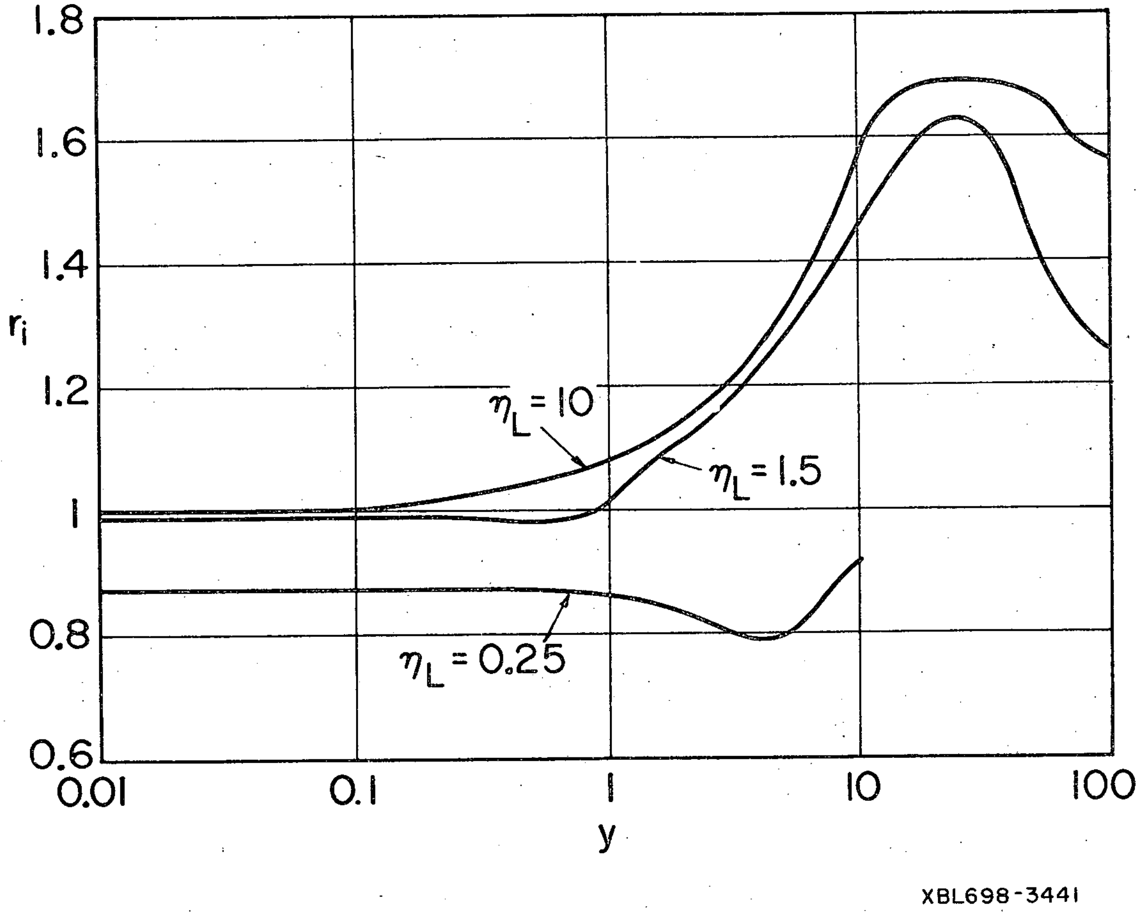
1.8
1.6
1.4
1.2
1
0.8
0.6
r_i
$\eta_L = 10$
$\eta_L = 1.5$
$\eta_L = 0.25$
0.01
0.1
1
10
100
y
XBL698-3441

Fig. 9

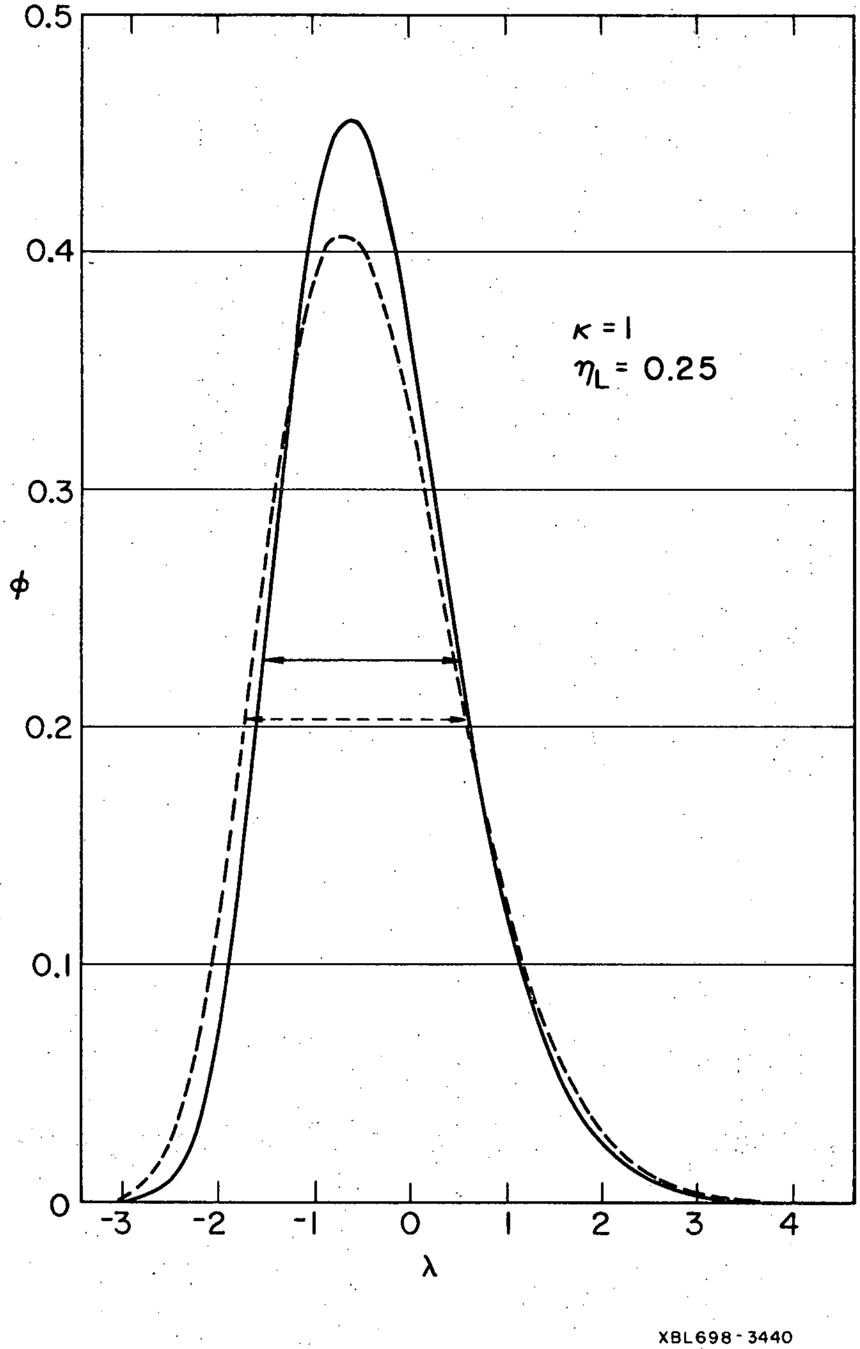

Fig. 10

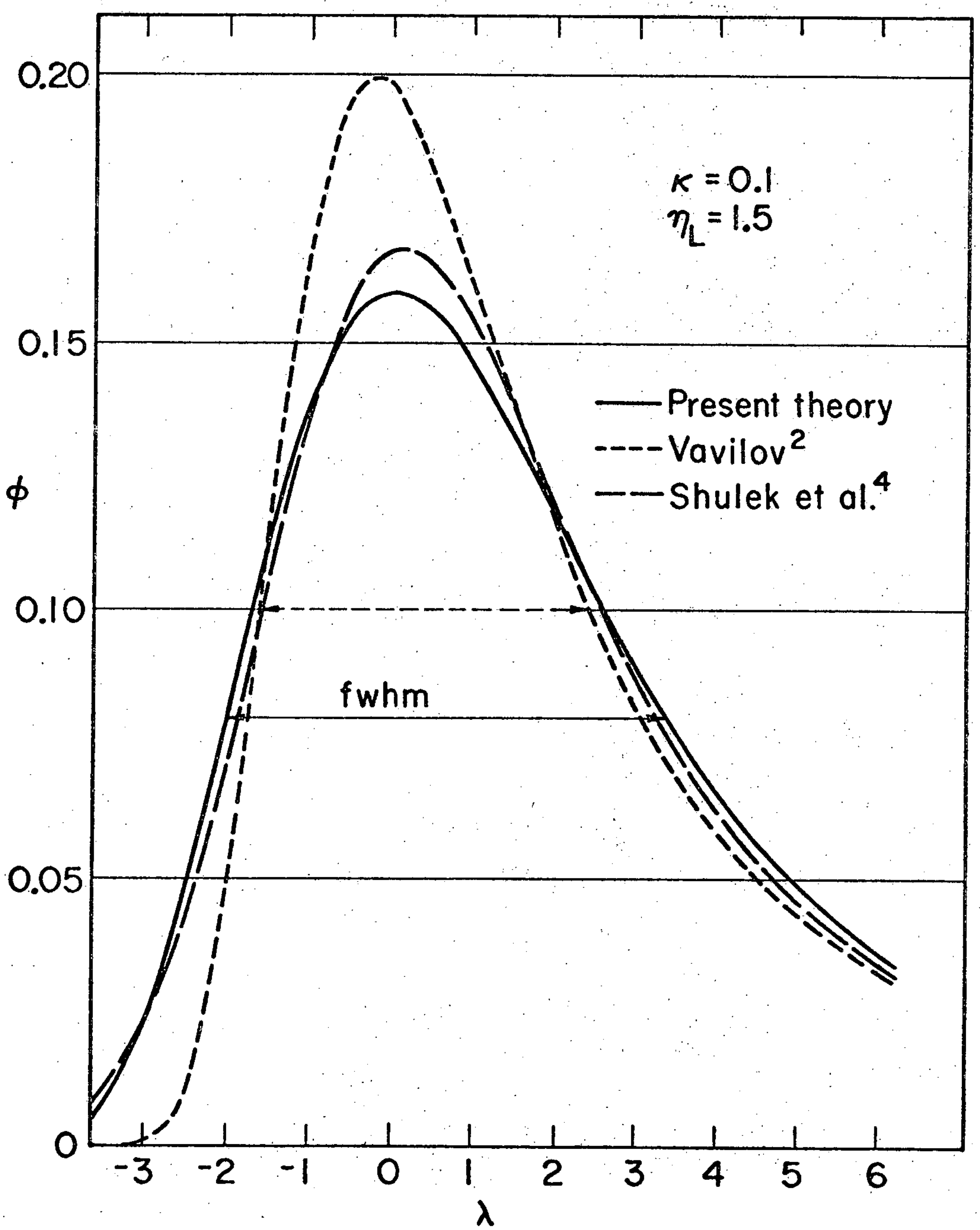

XBL698-3439

Fig. 11

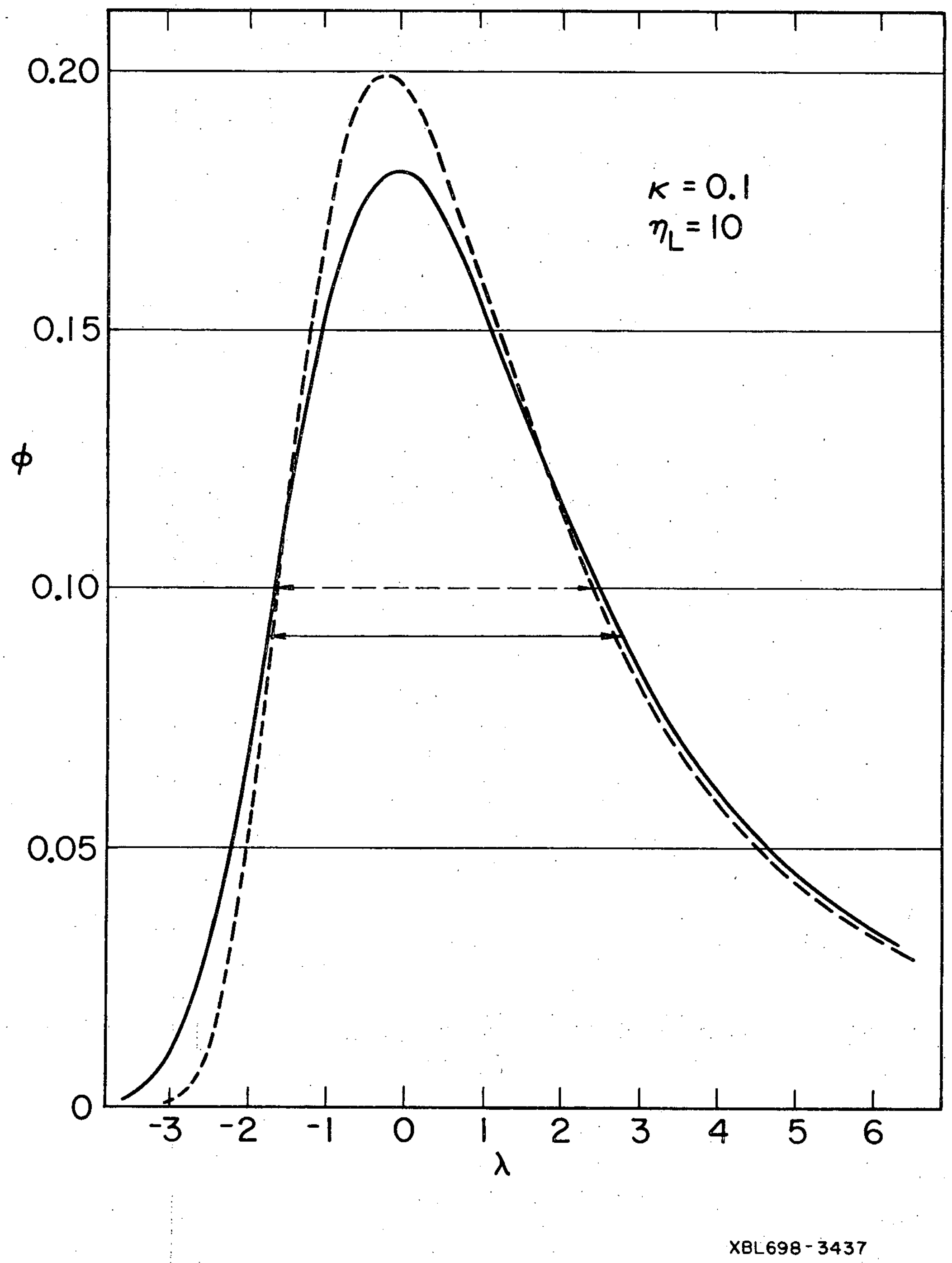
0.20
0.15
0.10
0.05
0
ϕ
$\kappa = 0.1$
$\eta_L = 10$
-3
-2
-1
0
1
2
3
4
5
6
λ
XBL698-3437

Fig. 12

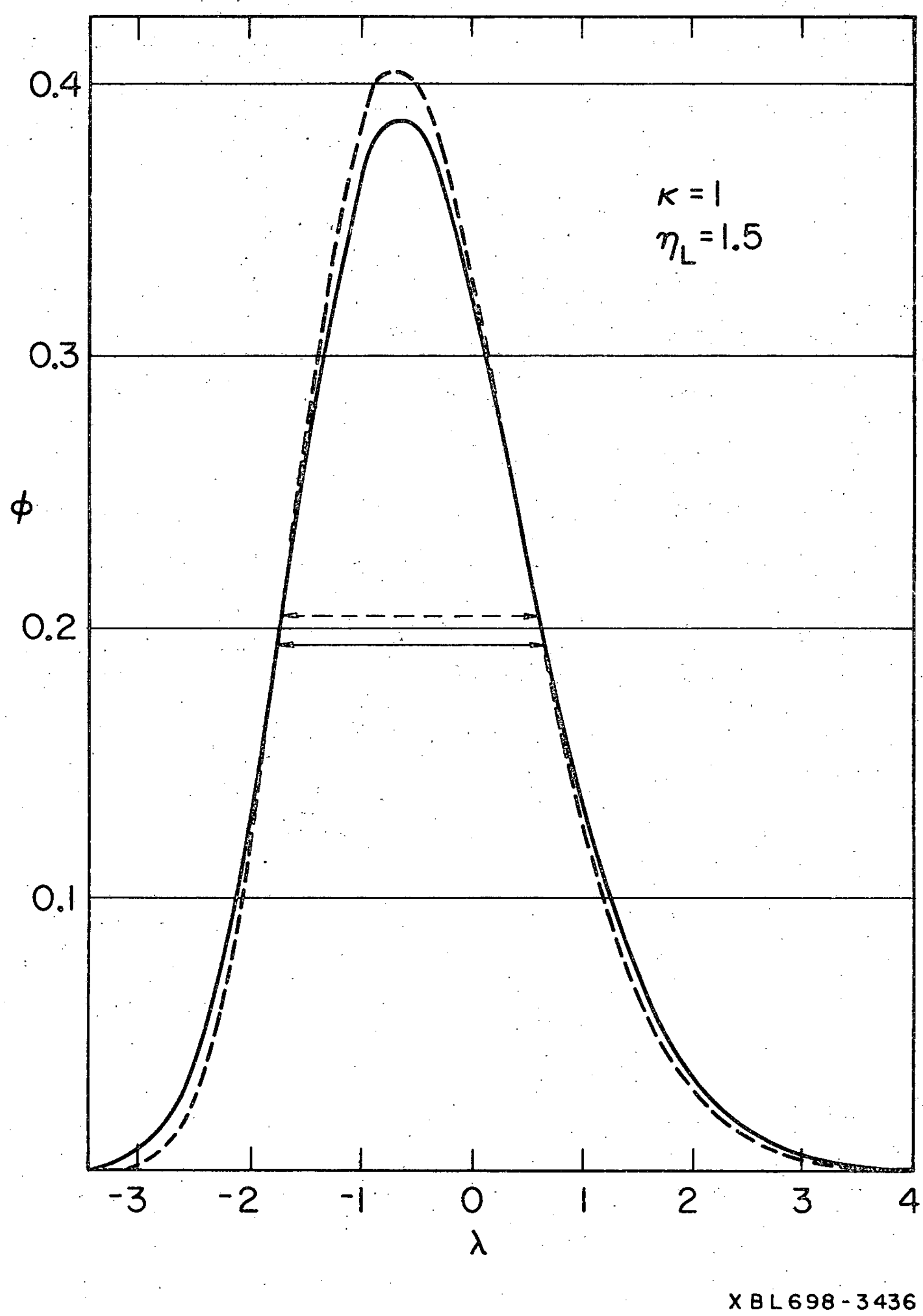

Fig. 13

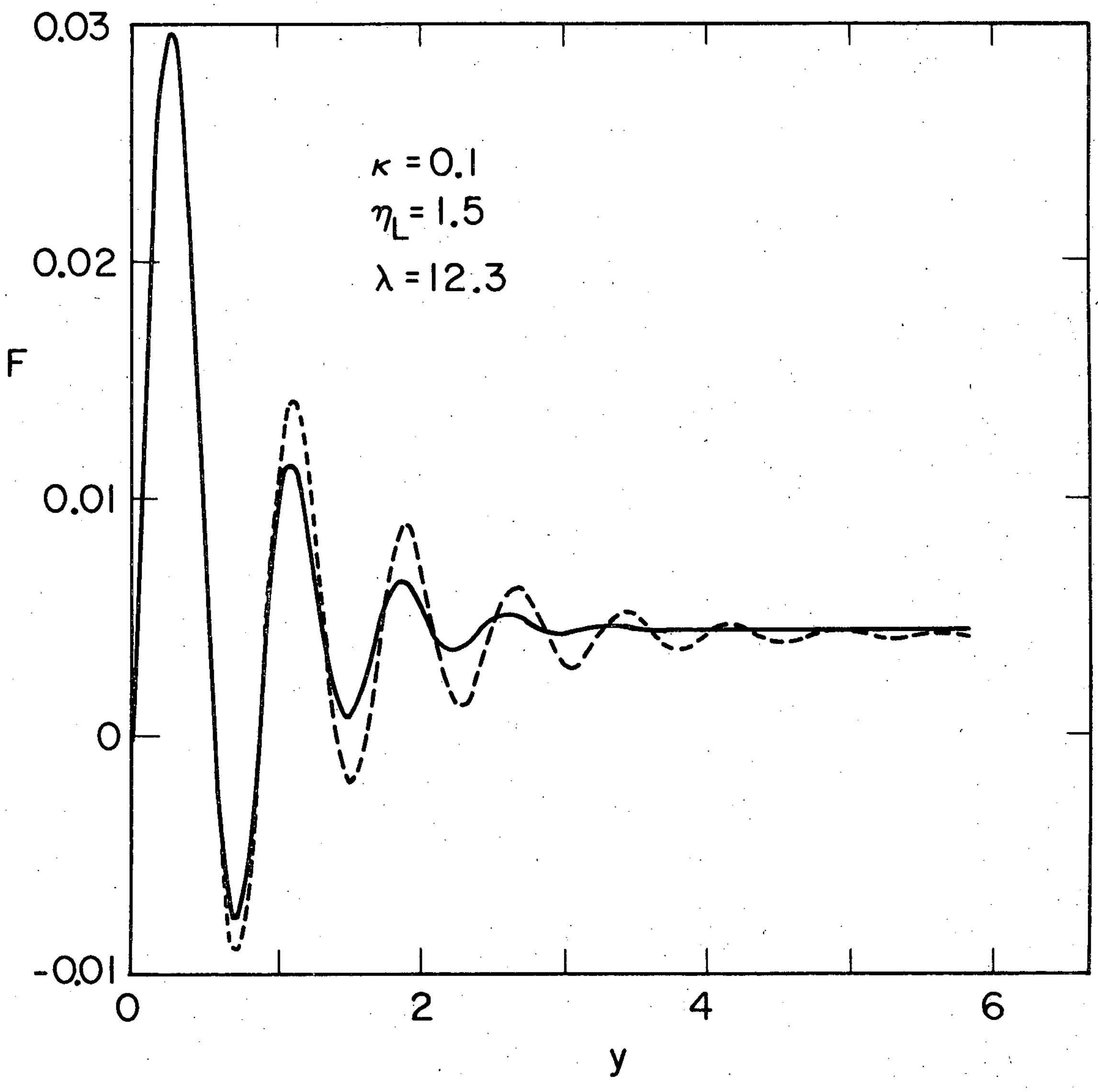

XBL698-3435

Fig. 14

TECHNICAL INFORMATION DIVISION
LAWRENCE RADIATION LABORATORY
UNIVERSITY OF CALIFORNIA
BERKELEY, CALIFORNIA 94720